Submitted to Physical Review Letters

LBL-4313
Preprint c.1

MOMENTS-OF-INERTIA IN ^{162}Yb AT VERY HIGH SPINS

R. S. Simon, M. V. Banaschik, P. Colombani,
D. P. Soroka, F. S. Stephens, and R. M. Diamond

September 1975

Prepared for the U. S. Energy Research and
Development Administration under Contract W-7405-ENG-48

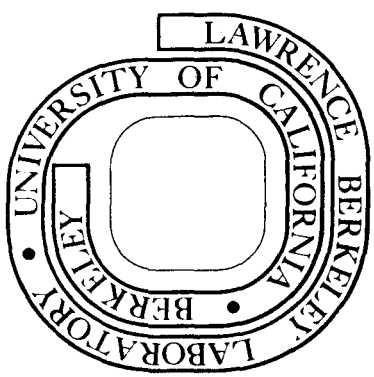

DISCLAIMER

LBL-4313

MOMENTS-OF-INERTIA IN ^{162}Yb AT VERY HIGH SPINS*

R. S. Simon,† M. V. Banaschik,‡ P. Colombani,§
D. P. Soroka, F. S. Stephens, and R. M. Diamond

Lawrence Berkeley Laboratory
University of California
Berkeley, California 94720

ABSTRACT

Two methods have been used to obtain values of the effective moment-of-inertia of very high-spin (20 - 50 ħ) states populated in heavy-ion compound-nucleus reactions. The ^{162}Yb nucleus studied has effective moments-of-inertia smaller than, but approaching, the rigid-body estimate.

It is now well established, that the gamma-ray spectrum following (HI,xn) reactions consists of a few discrete lines representing the last steps of the deexcitation process, and a continuum which contains the unresolved transitions between the preceding higher-energy, and higher-spin, states. Several studies of the continuum spectrum have recently been undertaken.[1-6] For medium to heavy product nuclei ($Z \gtrsim 50$), the continuum has two components: an exponential tail, and a lower-energy ($E \lesssim 2.5$ MeV) bump. The tail contains the first few statistical gamma rays emitted following the neutron evaporation. The bump contains the larger number of unresolved collective transitions that, together with the final discrete lines, carry off the large amount of angular momentum left in the product nucleus. The purpose of this work was to obtain nuclear moments-of-inertia at very high spins by studying the bump transitions in the final nucleus ^{162}Yb.

Two reactions were investigated: ^{150}Sm(^{16}O,4n)^{162}Yb and ^{126}Te(^{40}Ar, 4n)^{162}Yb. We measured the continuum spectrum in three 7.5×7.5 cm NaI(Tℓ) detectors at 0°, 45° and 90° with respect to the beam direction and 60 cm from the target. These detectors were gated by coincident pulses from a Ge detector at 225° to the beam and 5 cm from the target. The coincidence requirement with the Ge detector had two purposes: 1) to obtain the continuum spectrum associated with the 4n reaction channel by gating on discrete lines in ^{162}Yb, and 2) to provide a time signal to allow separation of pulses due to neutrons from those due to gamma rays based on their different flight time.

The energy distribution of the continuum gamma rays was obtained from the observed NaI pulse-height spectra by an unfolding procedure[7]

using a carefully adjusted response function and the measured total efficiency curve of the NaI detectors, with a small correction for the motion of the recoiling product nucleus. Comparison of the unfolded spectra from the different NaI detectors gives the angular distribution of the continuum gamma rays, whereas the sum of the three detectors (decreased by about 3%) gives the isotropic spectrum. By normalizing to the number of singles events in the gating lines of the Ge detector, the isotropic unfolded spectrum can be given in absolute events per decay and may be integrated to yield the average gamma-ray multiplicity, $\bar{N}_\gamma$, of the reaction. For the ^{40}Ar reaction at 181 MeV, raw and unfolded spectra are shown in Fig. 1, as well as the ratio of events at 0° to those at 90°.

To obtain $\bar{N}_\gamma$, we have summed the transitions in the unfolded spectrum above 0.34 MeV (the lowest energy considered to be reliable) and then added two transitions to represent the 0.166 MeV $2^+ \rightarrow 0^+$ and 0.320 MeV $4^+ \rightarrow 2^+$ lines of ^{162}Yb. The anisotropy (Fig. 1) suggests that most of the bump transitions are of stretched E2 character, so that an estimate of the average angular momentum, $\bar{\ell}$, in the channel can be obtained. Assuming no angular momentum is carried off by neutrons or the statistical cascade, we subtract the statistical transitions (all those in the exponential tail plus an estimated background underneath the bump — a total of $\sim$ 4 transitions in all cases) and multiply the rest by $2\hbar$. Both this estimated $\bar{\ell}$ and the total $\bar{N}_\gamma$ are given in Table 1. For the ^{16}O and low-energy ^{40}Ar cases, these $\bar{\ell}$ estimates are in excellent agreement with average values obtained from measured reaction channel cross sections, $\bar{\ell}(\sigma)$, using the sharp-cut-off model, as described previously.[1] Therefore, in these cases the upper boundary angular momentum, ℓ_u, given by the cross

section measurements seems very likely to be the maximum angular momentum in the yrast (collective) cascade. For the 181 MeV ^{40}Ar case the two $\bar{\ell}$ values do not agree, possibly indicating a net angular momentum carried by the neutrons and/or the statistical cascade. For our purposes the $\bar{\ell}$ based on the unfolded spectrum is more relevant, and the maximum angular momentum in the yrast cascade is estimated to be about 11 $\hbar$ larger than this $\bar{\ell}$ (based on the other two cases), giving a value of $\sim 50\hbar$. This number, however, is less certain than that for the other two cases.

There are two methods for obtaining effective moments-of-inertia, $\mathcal{J}$, from these data. One depends on relating a transition energy, E_t, to the corresponding spin, I, according to the approximate relation: $E_t = (\hbar^2/2\mathcal{J})(4I - 2)$. Both the raw and unfolded spectrum of Fig. 1 show a rather sharp upper edge of the bump. This edge is found to be lower for the ^{16}O and low-energy ^{40}Ar cases (shown schematically in the bottom part of Fig. 1) where less angular momentum is brought into the system. This suggests that the energies of the edge (given in Table 1) can be associated with gamma transitions between the highest spin states in the yrast cascade (estimated above). Three values for $2\mathcal{J}/\hbar^2$ can be obtained in this way and are plotted on Fig. 2 against $(\hbar\omega)^2$ in the usual backbending type of plot, where $\hbar\omega$ is taken to be $E_t/2$. Also shown are the moments-of-inertia of the known low-spin states in ^{162}Yb and, for comparison, the low-spin data for the isotone ^{160}Er.

The same method can be applied for transitions in a region of the spectrum corresponding to ℓ values below which there is no appreciable direct population into the channel of interest. This region is likely to be below 30 - 35 $\hbar$ for the 4n channel in the 181 MeV ^{40}Ar case (Fig. 1)

since most of the population with lower spins goes into the 5n or 6n channels, but it would be less than 20 $\hbar$ for the ^{16}O and low-energy ^{40}Ar cases. Provided there is a monotonic increase of transition energy with spin (no backbending), a spin value for each transition energy can be obtained by summing all the transitions (less the estimated statistical cascade background) up to that transition energy and multiplying by two. This method is applicable between $\sim$ 0.7 and 1.0 MeV in Fig. 1, leading to moments-of-inertia given by the dots connected by a solid line in Fig. 2.

The preceding method is an "integral" one, and thus is not very sensitive to local variations in the moment-of-inertia. The second method is a "differential" one, and can show such local variations. Each point on the unfolded spectrum of Fig. 1 gives the number of transitions per 40 keV energy interval. The reciprocal of this is the difference, ΔE_t, between transition energies and is related to the moment-of-inertia by

$$\Delta E_t \approx \frac{8\hbar^2}{2\mathcal{J}} - 2E_t \frac{d\ell n \mathcal{J}}{dI} \qquad (1)$$

where E_t is the transition energy for which ΔE_t is evaluated. This method also requires the full population in the channel, and thus can only be applied below 30 - 35 $\hbar$ for the 181 MeV ^{40}Ar case. For the region 0.7 - 1.0 MeV in Fig. 1, $\mathcal{J}$ is nearly constant, so that the last term of Eq. (1) can be neglected, giving $2\mathcal{J}/\hbar^2 \approx 8/\Delta E_t$. This procedure leads to the diamonds and dashed line in Fig. 2. The results are in good agreement with those of the integral method and suggest that there might be a local increase in the moment-of-inertia around $(\hbar\omega)^2 \sim 0.2$ MeV^2 or $E_t \sim 0.9$ MeV. This possible rise can be seen directly in both the

unfolded and raw spectra of Fig. 1, but it is not clearly outside the present uncertainty limits. The power of this method is that changes in the moment-of-inertia can be recognized directly from irregularities in the spectrum, thereby providing a simple means to pick out regions of particular interest. In addition, it is possible to derive independent spin values using the moments-of-inertia obtained from this method and the corresponding transition energies.

The effective moment-of-inertia values measured by the techniques described above are compared in Fig. 2 with that of a rigid diffuse sphere of mass 162, having an equivalent r.m.s. radius of 6.71 fm.[8] The deformed rigid-body value for the moment-of-inertia would be roughly 10% larger than this rigid-sphere value. The data above spin 20 — $(\hbar\omega)^2 \sim 0.12$ MeV^2 — are nearly consistent with the rigid-sphere value, but seem likely to be below the deformed value at least up to spin ~ 40 — $(\hbar\omega)^2 \sim 0.35$ MeV^2. Since ^{162}Yb is almost surely deformed, this might indicate that there are still some pairing correlations (or other effects) at these spin values which reduce the effective moment-of-inertia below the rigid-body value. It will obviously be of interest to improve these methods in order to see more details of these moments-of-inertia and to extend the measurements to other nuclei.

TABLE 1. Data used to obtain moments-of-inertia.

Reaction	E_{proj} MeV	$\bar{N}_\gamma$	$\bar{\ell}$ ħ	E_{edge} MeV	$\sigma(4n)$ mbarn	$\sum_{x=4}^{6} \sigma(xn)^a$ mbarn	$\ell_u(4n)$ ħ	$\bar{\ell}(\sigma)^b$ ħ
$^{150}Sm + ^{16}O$	87	17	26	1.12	540	760	36	27
$^{126}Te + ^{40}Ar$	157	17	27	1.16	220	280	39	28
$^{126}Te + ^{40}Ar$	181	23	39	1.40	220	620	63	56

[a] Includes 15% for charged-particle channels. In the 5n reaction the measured $i_{13/2}$ band population was increased by 35% to allow for other bands.

[b] $\bar{\ell}(\sigma) = 0.67[\ell_u^3(4n) - \ell_u^3(5n)] / [\ell_u^2(4n) - \ell_u^2(5n)]$

FOOTNOTES AND REFERENCES

*This work was done under the auspices of the U. S. Energy Research and Environmental Administration.

†On leave from Sektion Physik der Ludwig-Maximilians-Universität München, 8046 Garching, Germany; sponsored by the Bundesministerium für Forschung und Technologie.

‡Present address: Technische Hochschule, Darmstadt, Germany.

§Permanent address: Institut de Physique Nucléaire, 91406 Orsay, France.

1. P. Tjøm, F. S. Stephens, R. M. Diamond, J. de Boer, and W. E. Meyerhof, Phys. Rev. Letters 33, 593 (1974).
2. E. der Mateosian, O. C. Kistner, and A. W. Sunyar, Phys. Rev. Letters 33, 596 (1974).
3. J. O. Newton, J. C. Lisle, G. D. Dracoulis, J. R. Leigh, and D. C. Weisser, Phys. Rev. Letters 34, 99 (1975).
4. M. Fenzl and O. W. B. Schult, Z. Physik 272, 207 (1975).
5. M. V. Banaschik, R. S. Simon, P. Colombani, D. P. Soroka, F. S. Stephens, and R. M. Diamond, Phys. Rev. Letters 34, 892 (1975).
6. G. B. Hagemann, R. Broda, B. Herskind, M. Ishihara, S. Ogaza, and H. Ryde, Nucl. Phys. A245, 166 (1975).
7. J. F. Mollenauer, Lawrence Radiation Laboratory Report UCRL-9748 (1961).
8. W. D. Meyers, Nucl. Phys. A204, 465 (1973).

FIGURE CAPTIONS

Fig. 1. Raw (□) and unfolded (●) continuum gamma spectra from the $^{126}Te(^{40}Ar,4n)^{162}Yb$ reaction at 181 MeV. The larger solid dots represent 5 channel averages. Also shown is the 0/90 ratio for the unfolded spectrum. At the bottom are schematic spectra for this case (solid line), the $^{126}Te(^{40}Ar,4n)^{162}Yb$ reaction at 157 MeV (longer-dashed line) and the $^{150}Sm(^{16}O,4n)^{162}Yb$ reaction at 87 MeV (shorter-dashed line).

Fig. 2. Backbending plot for ^{162}Yb. The small solid dots correspond to the known low-spin states of ^{162}Yb, whereas the open circles are for the isotone ^{160}Er. The large dots correspond to values derived by the integral method from the 181 MeV ^{40}Ar data. The triangle and square come from the 157 MeV ^{40}Ar and 87 MeV ^{16}O spectra using the same method. The diamonds are values from the differential method applied to the 181 MeV ^{40}Ar case. The horizontal dashed line is the moment-of-inertia of a rigid sphere with A = 162.

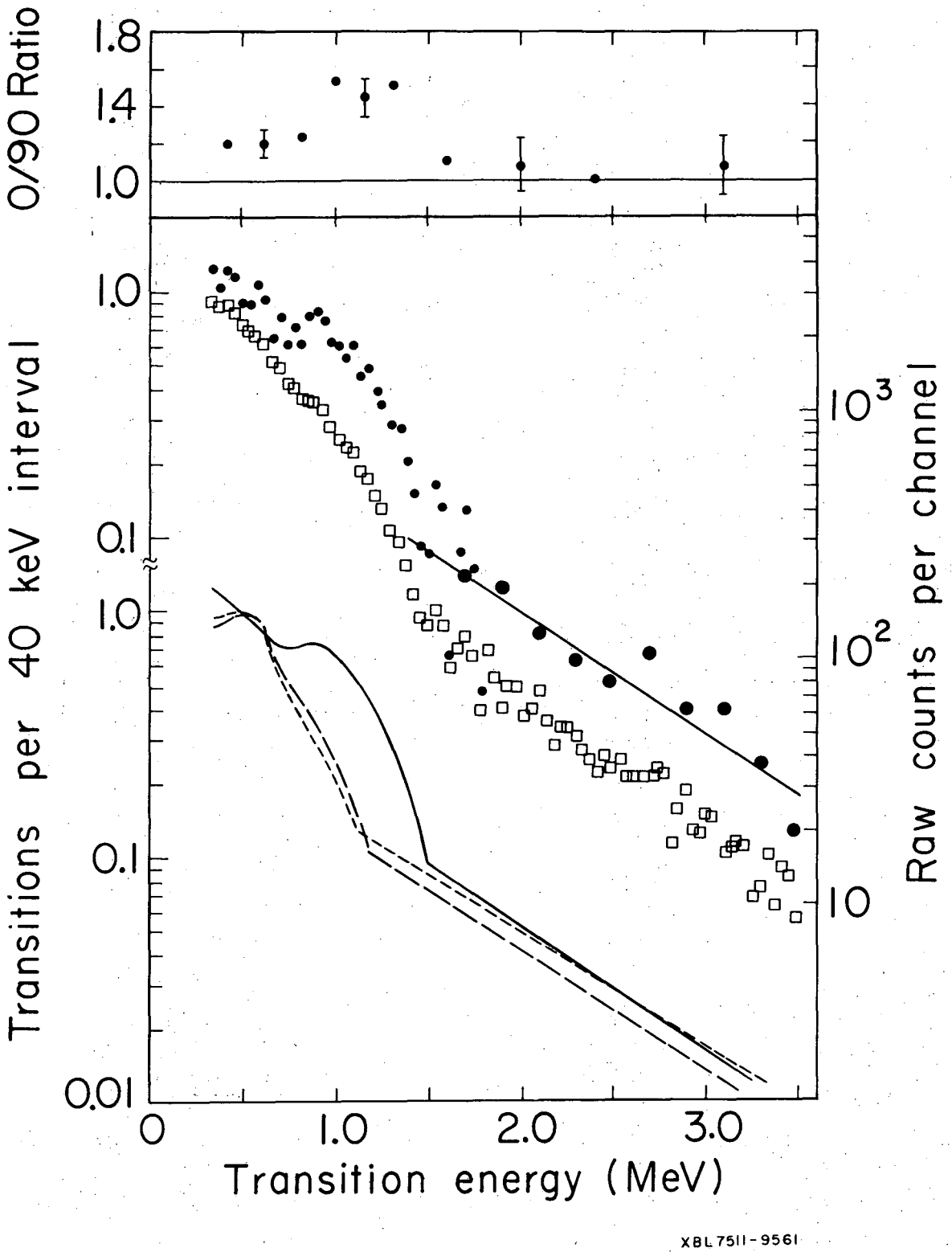
0/90 Ratio
1.8
1.4
1.0
Transitions per 40 keV interval
1.0
0.1
1.0
0.1
0.01
Raw counts per channel
10^3
10^2
10
0
1.0
2.0
3.0
Transition energy (MeV)
XBL7511-9561

Fig. 1

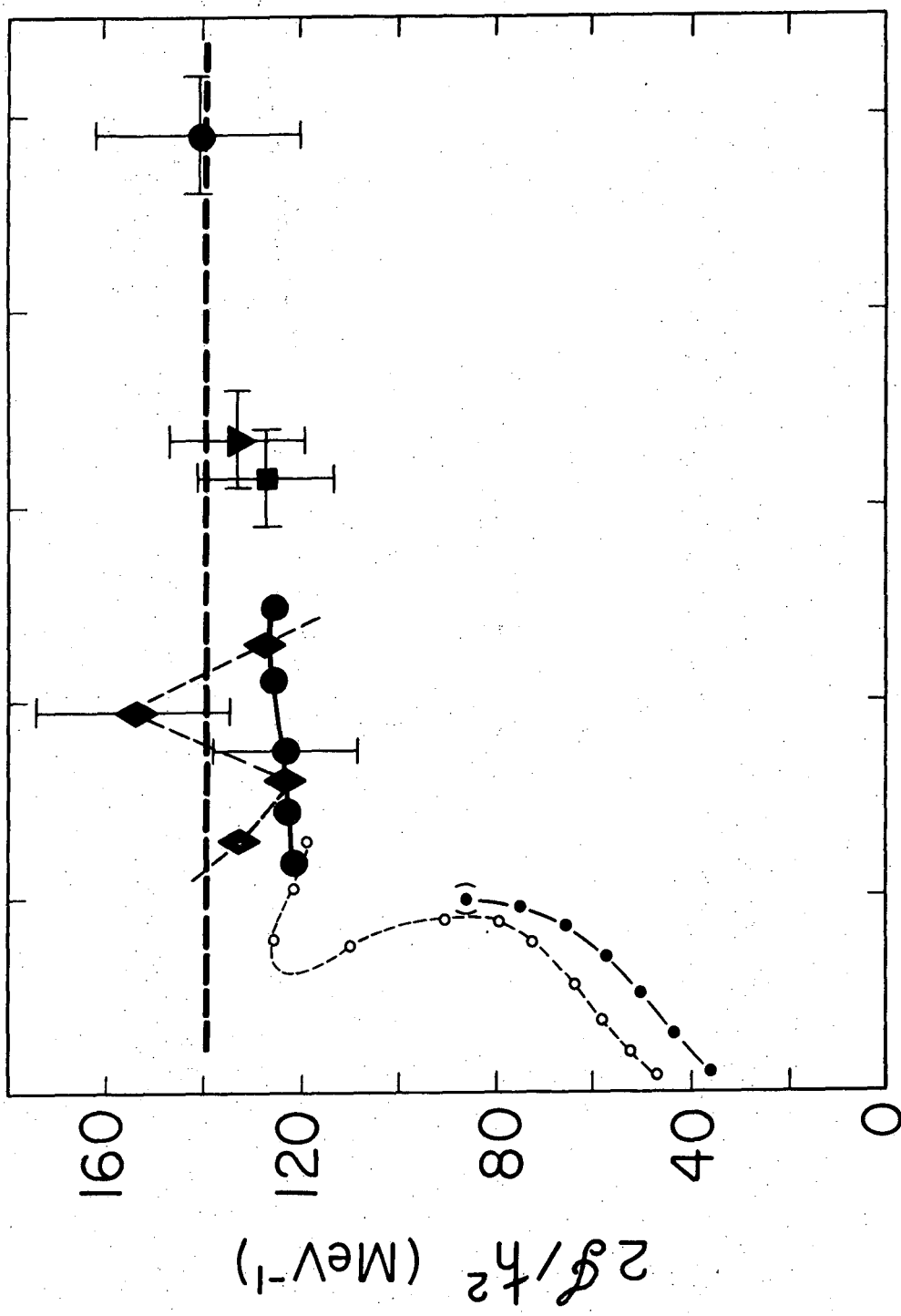

XBL7511-9562

Fig. 2

TECHNICAL INFORMATION DIVISION
LAWRENCE BERKELEY LABORATORY
UNIVERSITY OF CALIFORNIA
BERKELEY, CALIFORNIA 94720